THE ASTROPHYSICAL JOURNAL, 272:223–233, 1983 September 1

OUTER ATMOSPHERES OF COOL STARS. XIII. CAPELLA AT CRITICAL PHASES

THOMAS R. AYRES[1]
Laboratory for Atmospheric and Space Physics, University of Colorado
FRANCIS H. SCHIFFER III[1]
Astronomy Department, Computer Sciences Corporation
AND
JEFFREY L. LINSKY[1,2]
Joint Institute for Laboratory Astrophysics, University of Colorado and National Bureau of Standards
Received 1982 December 2; accepted 1983 February 18

ABSTRACT

We present a high-dispersion ultraviolet study of the late-type spectroscopic binary Capella covering critical phases—three quadratures and one conjunction—in the orbit, as observed with the *International Ultraviolet Explorer*. Our work supports the conclusion previously reached by Ayres and Linsky, based on an early *IUE* study of Capella with limited phase coverage, that the rapidly rotating F9 III secondary star in the system is considerably brighter than the more slowly rotating G6 III primary in ultraviolet emission lines characteristic of the chromospheric ($T \sim 6000$ K) and higher temperature ($T \lesssim 2 \times 10^5$ K) plasmas. In particular, the secondary is responsible for about 90% of the C IV (10^5 K) emission from the system, and the secondary/primary surface flux ratio is as large as 25:1. However, the present study reveals that the primary star nevertheless is among the brightest of the yellow giants in C IV surface flux, and perhaps is responsible for a significant fraction of the soft X-ray emission from the system.

The enhanced ultraviolet emission of the Capella gaints compared to other yellow giants in recent *IUE* low-dispersion surveys suggests that the primary and secondary both are crossing the Hertzsprung gap for the first time, as proposed previously by Boesgaard in her examination of the lithium absorption in the composite spectrum. If the Capella giants indeed are both first crossers, then the spin-down of stars evolving through the Hertzsprung gap may be quite rapid, as has been suggested on theoretical grounds by Endal and Sofia. In fact, the rotational velocities measured for the Capella giants by Fekel are consistent with the angular momentum histories of yellow giants in the Hertzsprung gap predicted by Gray and Endal in their study of the four more evolved Hyades K giants. We conclude that the extraordinary brightness of the Capella secondary in the far-ultraviolet is a transitory, dynamic magnetic phase in the post–main-sequence evolution of moderately massive ($\sim 3\ M_\odot$) stars.

Subject headings: stars: binaries — stars: chromospheres — stars: individual — stars: late-type — ultraviolet: spectra

I. INTRODUCTION

One of the most unusual stellar systems in the solar neighborhood is the spectroscopic binary Capella (α Aurigae A; G6 III[Aa] + F9 III([Ab]). Both components are nearly identical in mass, luminosity, temperature, radius, and presumably also age and chemical composition, but visible and ultraviolet spectra of the pair differ remarkably. On the one hand, the optical spectrum of the primary is sharp-lined, while that of the secondary is diffuse and difficult to identify (Wright 1954), aside from an unusually strong Li I λ6708 absorption (Wallerstein 1966). On the other hand, the far-ultraviolet emission spectrum of the secondary is quite prominent, while that of the primary is difficult to detect (Ayres and Linsky 1980).

Iben (1965) proposed an explanation for the lithium richness and spectral diffuseness of the secondary. He suggested that the primary is a slowly rotating, post-helium-flash yellow giant, while the secondary is crossing the Hertzsprung gap for the first time. Accordingly, the F giant still is shedding the substantial angular momentum inherited from its rapidly rotating late B or early A main-sequence progenitor, and still is burning its primordial surface lithium by deep mixing. Furthermore, the fast rotation of the secondary coupled with its recent development of a convection zone very likely produces intense magnetic activity through vigorous dynamo action (Parker 1970), a manifestion of which is the bright chromosphere and corona seen in the ultraviolet and soft X-ray bands (e.g., Vaiana and Rosner 1978). Accordingly, the Capella giants provide important prototypes for testing theoretical concepts of stellar evolution, the origin of magnetic activity, and the

[1] Guest Observer, *International Ultraviolet Explorer*.
[2] Staff Member, Quantum Physics Division, National Bureau of Standards.

development of chromospheres and coronae on late-type stars.

Here, we present the results of a program of high-dispersion spectroscopy of Capella at critical orbital phases utilizing the *International Ultraviolet Explorer* (Boggess *et al.* 1978). The objective of the program was to establish as carefully as possible the relative ultraviolet emission levels of the Capella primary and secondary in order to gain insight concerning the nature of their chromospheres and coronae.

II. OBSERVATIONS

a) *Observing Program*

A useful strategy for isolating the emission from each component of a spectroscopic binary is to observe the system at opposite quadratures (maximum velocity separation) as well as at the conjunctions (single-line phase) (Wright 1954; Boesgaard 1971). Accordingly, we observed Capella at, or near, phases 0.25, 0.50 and 0.75 of one orbit in the spring of 1980, and near phase 0.25 of a subsequent orbit in early 1981.[3] Owing to scheduling constraints, it was not always possible to observe at precisely the desired orbital phase, but in no case did the difference between actual and target phases exceed 0.02 cycles.

[3] We adopt the following ephemeris for Capella based on that cited by Batten, Fletcher, and Mann (1978): JD = 2,442,093.4 $\pm$ 0.2 + 104.0204E, where phase 0.0 is the conjunction with the more massive star, the G6 III primary, in front.

Our goal was to acquire high signal-to-noise ultraviolet spectra at each critical orbital phase in order to characterize the properties of low-excitation and high-excitation emission lines as a function of the differential radial velocities of the two giants. In addition, we intended to search for short-term variability in the Capella spectrum, produced by flare activity on the secondary star for example. To accomplish these objectives we devoted an entire 8 hour shift at each observing opportunity to sequential echelle exposures, alternating between the SWP (1150–2000 Å) and LWR (2000–3000 Å) cameras. Typical exposure times were 30 minutes for the far-ultraviolet region and 1 minute for the middle-ultraviolet, through the large aperture (10″ × 20″) in both cases. A catalog of the observations is provided in Table 1.

During the first observing opportunity, at orbital phase 0.26, we also obtained two small-aperture (3″ diameter) spectra of Capella, a 60 minute SWP and a 2 minute LWR exposure, in conjunction with wavelength calibration exposures in both spectrographs utilizing the on-board platinum hollow-cathode emission line lamp. During the second opportunity, at phase 0.52 of the same orbit, we included two 10 minute SWP exposures to provide unsaturated profiles of the bright Si III] λ1892 emission feature. (Unfortunately, the first of the 10 minute exposures, SWP 8626, is affected by a strong cosmic ray hit at λ1892 and therefore was not usable.) The third opportunity, at phase 0.76 of that orbit, consisted solely of interleaved 30 minute SWP and

TABLE 1

CATALOG OF OBSERVATIONS

JD 2,444,000+ (mid-shift)	Orbital Phase[a] (mid-shift)	Image Numbers[b]	Exposure Times (minutes)
305.5	0.27	SWP 8178	30
		8179[c]	60
		8180[c]	wavecal
		8181–8183	30
		LWR 7107, 7108	1
		7109[c]	wavecal
		7110[c]	2
		7111, 7112	1
331.4	0.52	SWP 8626	10
		8627	30
		8628–8631	25
		8632	10
		LWR 7371–7377	40 s
356.4	0.76	SWP 8832–8838	30
		LWR 7616, 7617	1
		7618–7623	55 s
616.6	0.26	SWP 11028	60
		11030	10
		11032	60
		11033	55
		LWR 9695, 9696	1

[a] JD = 2,442,093.4 $\pm$ 0.2 + 104.0204E, phase 0.0 is the conjunction with the more massive star (G6 III) in front (from Batten, Fletcher, and Mann 1978).

[b] SWP spectral range: 1150–2000 Å; LWR spectral range: 2000–3000 Å. All exposures through 10″ × 20″ aperture unless otherwise indicated.

[c] Small aperture (3″ diameter); "wavecal" refers to a wavelength calibration exposure utilizing the platinum hollow-cathode emission-line lamp.

1 minute LWR exposures for the entire 8 hour shift. During the final opportunity, at phase 0.26 of a subsequent orbit, we increased the SWP exposures to 60 minutes for three spectra, and obtained a 10 minute SWP spectrum to record the Si III] feature. In addition, we took two low-dispersion SWP spectra, 1 minute and 6 minute exposures, for use in a high-dispersion calibration effort that will be reported elsewhere (Ayres 1983*a*).

b) *Reduction to Absolute Flux*

We reduced the *IUE* echellograms utilizing the extracted-spectrum (ESHI) file of the Guest Observer tapes, as follows:

We heavily smoothed the interorder backgrounds with a 100 point running mean to eliminate particle radiation hits, camera artifacts, and reseau marks at the scale of the emission line widths, but retain gross structure of the background, like curvature across the order. We then subtracted the smoothed background from the on-order gross spectrum, and corrected the resulting net spectrum for the echelle blaze using the sinc plus parabolic term algorithm (*IUE* Image Processing Information Manual, Version 1.0, p. 6.10), with the order-dependent grating constants derived by Beeckmans and Penston (1979). Finally, we divided the blaze-corrected spectrum by the exposure time and multiplied by a logarithmically interpolated inverse sensitivity function based on the provisional high-dispersion calibration for sharp-line emission sources proposed by Cassatella, Ponz, and Selvelli (1981). (We caution that the flux scale based on that calibration may be somewhat low shortward of 1500 Å; see Ayres 1983*a*).

Because they are important in the chromospheric radiative energy budget, we treated the Lyα λ1216 feature and the Mg II $\lambda\lambda$2796, 2803 doublet in greater detail. The background at Lyα is enhanced artificially by the spillover of both stellar and geocoronal emission into the interorder region. We therefore synthesized a background by interpolating linearly between the mean signal in a 25 point band near the camera edge and a 100 point band near the center of the extracted order, well away from the contaminated region. We then corrected the net spectra for the echelle blaze by adjusting the grating constant to equalize the fluxes in a wavelength bandpass common to the adjacent orders in which the Lyα emission appears (m = 114, 113). We calibrated the resulting blaze-corrected spectra in the manner described previously. We also corrected the Mg II h and k features by a similar technique, although it was not necessary to modify the original backgrounds since the echelle orders are well separated at that end of the LWR format.

c) *Superposition of Spectra*

At each observing session, we accumulated as many as seven high-dispersion spectra from each camera. In order to obtain composite profiles with higher signal-to-noise, we co-added the individual spectra on a common wavelength scale. At the same time, we calculated the rms deviation of the individual spectra from the composite, point by point. The rms spectrum will contain structure when, for example, a bright cosmic ray hit appears in one exposure at a particular wavelength but not in the other exposures. We used this property to identify and delete the brightest hits in the individual spectra. The rms record also will contain structure when a sharp emission line is not properly registered in wavelength in one exposure compared with the others, owing to thermal shifts of the echelle format, for example. Fortunately, the camera temperatures were reasonably stable during each observing sequence, and there is little evidence for misregistrations in the composite spectra. Finally, the rms record provides a convenient means to judge the reality of any feature or structure in the composite spectra. In this manner, we identified a number of persistent emission spikes in one of the well-exposed lines—C IV λ1548—that appear to be stationary in the reference frame of the spectrograph, and therefore likely are camera artifacts ("warm" pixels akin to the well-known λ2200 "hot" pixel of the LWR camera).

d) *Velocity Scales*

For interpreting orbital variations in the emission profiles, the assignment of a reliable velocity scale is critical. Unfortunately, this was the most formidable challenge of our analysis, owing to the way in which the *IUE* echelle images were processed during the epoch of observation. Prior to 1980 July 18, wavelength scales were assigned according to dispersion constants that were updated by biweekly platinum lamp calibration exposures. At that time, the large velocity errors that can be produced by thermal flexing of the spectrographs (e.g., Turnrose, Thompson, and Bohlin 1982) were not fully appreciated. Consequently, if the biweekly wavelength calibration were obtained at a very different temperature from that of a science exposure, a systematic, and often large, wavelength error could be introduced. Furthermore, velocity shifts are always possible in large-aperture spectra owing to the positional uncertainty of the target in the slot.

We did, however, obtain small-aperture spectra in both cameras at phase 0.27 which can be placed on an absolute wavelength scale using the nearly contemporaneous platinum lamp exposures. (These were extracted using the same dispersion constants as were applied for the stellar spectra.) In addition, the emission features of the single-lined spectrum taken near the phase 0.5 conjunction should be close to the accurately measured center-of-mass (COM) velocity of the system (v_R = +29.5 km s^{-1}; see Batten, Fletcher, and Mann 1978). We utilized the two "absolute" velocity measures to calibrate "secondary" velocity indicators that appear in all of the spectra, including the prominent interstellar Lyα absorptions of H I and D I in the far-ultraviolet region, and the interstellar Mg II h and k absorptions in the middle-ultraviolet region.

We reduced the platinum lamp spectra in the same manner as the stellar exposures, and measured line positions using a least-squares Gaussian fitting procedure. We examined 12 echelle orders in the SWP wavecal corresponding to those containing emission lines of interest in the stellar spectra. The mean velocity of the orders, based on the rest wavelengths of the platinum calibration lines published by Turnrose and Bohlin (1981), is -7.0 ± 1.0 km s^{-1}, where the uncertainty is the standard error of the mean (12 orders). The standard deviation of the mean values for each order about the cumulative mean is 3.5 km s^{-1}, and the typical standard deviation of the individual velocities about the mean in a single order is about 3 km s^{-1} (for those orders containing four or more calibration lines). The latter value very likely is representative of the single-measurement random error for well-exposed, narrow emission lines. The orders exhibiting the largest deviations from the mean velocity ($m = 106$, 113) occur in the short-wavelength end of the SWP format where the platinum spectrum is sparse and faint.

In the LWR image, we measured the platinum lines in the three orders, 82–84, that bracket the Mg II h and k doublet. The mean velocity of the three orders is -5.1 ± 0.8 km s^{-1}, where again the uncertainty is the standard error of the mean. The standard deviation of the individual orders about the mean, as well as the standard deviation of platinum line velocities about the mean in each order, is ~ 1.5 km s^{-1}.

For both wavelength regions, we applied the velocity corrections indicated by the platinum spectra order-by-order to obtain absolute velocities for the stellar emission lines. We also compensated for the heliocentric motion of the Earth at the time of observation, but did not correct for the projected satellite motion, which was negligible ($\lesssim 1$ km s^{-1}).

Next, we examined the composite Lyα and Mg II emission profiles observed near the single-lined phase 0.5 conjunction, when the velocities of the Capella giants coincide with that of the system center of mass. We determined a velocity of -8 ± 3 km s^{-1} for the interstellar Mg II components relative to the emission centroids of the stellar h and k lines, where the cited uncertainty ($\pm 1\ \sigma$) is based on the standard deviation of measurements applied to the individual h and k profiles that ultimately were combined into the composite profiles. If the outer edges of the Mg II emission cores reliably indicate the system velocity at phase 0.52, then the Mg II interstellar velocity is $+22 \pm 3$ heliocentric. This value is compatible with previously published D I Lyα velocities based on *Copernicus* observations of Capella by Dupree, Baliunas, and Shipman (1977), but is somewhat larger than would be expected for Capella's line of sight based on the interstellar flow vector cited by Böhm-Vitense (1981). The interstellar Mg II velocity inferred from the phase 0.52 spectrum also is compatible with the absolute velocity indicated by the phase 0.27 small-aperture spectrum of the k line, although the interstellar feature is not as clearly visible as in the more deeply exposed large-aperture spectra. (However, the lower signal-to-noise, small-aperture profile of the h line exhibits a deeper, more violet-displaced absorption than the k line.)

Accordingly, for the phase 0.26, 0.27, and 0.76 quadrature composite profiles, we registered the velocity scales according to the apparent position of the Mg II k interstellar absorption feature and the interstellar medium velocity cited above. However, owing to the phase-dependent distortions of the stellar Mg II emission envelope against which the interstellar absorption must be viewed, the registration procedure probably is accurate to no better than ± 5 km s^{-1}.

Figure 1 compares the composite profiles of Mg II h and k at the four orbital phases. The profiles are

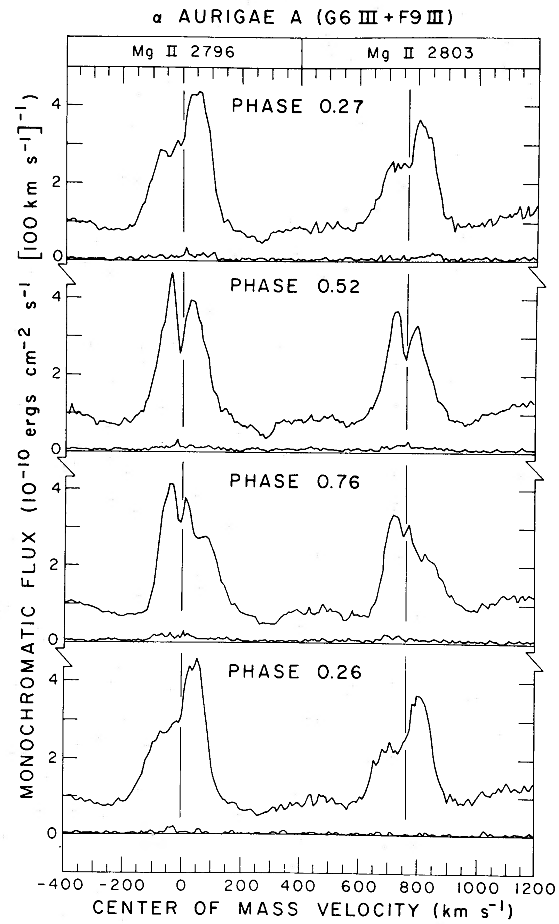

FIG. 1.—Mg II h (λ2803) and k (λ2796) resonance lines of Capella system as a function of orbital phase. The ordinate is the monochromatic flux measured at Earth in units compatible with the segmented velocity scale of the abscissa. Each spectrum is a superposition of up to seven individual LWR exposures. The tracing immediately above the zero level in each panel is the rms deviation of the individual profiles from the composite, point by point. The vertical tick marks indicate zero velocity in the reference frame of the system center of mass. Capella Ab (secondary star) is to the short-wavelength side (negative velocities) of the COM at the phase 0.25 quadrature ($V_{\rm Ab} \approx -26$) while Capella Aa (primary star) is to the long-wavelength side ($V_{\rm Aa} \cong +27$). At the phase 0.5 conjunction, Capella Aa and Ab both are at the system center of mass velocity, and at the phase 0.75 quadrature, the component velocities are reversed from those at phase 0.25. The stationary absorption features near -8 km s^{-1} at all phases are the interstellar Mg II components that were used to register the individual composite spectra to the COM velocity frame.

depicted on a monochromatic flux scale with units compatible with those of the velocity scale of the abscissa. Vertical tick marks indicate the rest velocity of the lines in the system center-of-mass frame. Note the stationary (in center-of-mass velocity) interstellar absorption components that were used to register the quadrature velocity scales to that of the conjunction spectrum. The gross distortion of the Mg II profiles with the orbital motion of the Capella giants is clearly evident.

In the far-ultraviolet region, the bright stellar Lyα emission is heavily absorbed near line center by interstellar neutral hydrogen. On the shortward flank of the broad H I absorption core is a weak absorption feature due to interstellar deuterium Lyα. We used the overall shape of the combined H I + D I absorption to provide a velocity reference for the far-ultraviolet spectra. Other interstellar features are also likely to be present in the 0 cm^{-1} lower level lines of O I (λ1302) and C II (λ1335) (cf. Ayres *et al.* 1983). Unfortunately, reseau marks fall on both features in the large-aperture spectra, and prevent their use for registration purposes.

In practice, we numerically cross-correlated the Lyα absorption cores of the quadrature profiles against that of the conjunction profile, which was adjusted to the center-of-mass velocity frame using the flux-weighted mean positions of the low-excitation O I λλ1305, 1306 and Si II λ1808 features (cf. Ayres and Linsky 1980). We cross-correlated both the unaltered absorption cores and "rectified" absorption cores obtained by folding out a least-squares Gaussian profile that was fitted to the outer emission wings of Lyα well away from the interstellar absorption core. The second procedure crudely accounts for the influence of the intrinsic stellar emission profile, which, like *h* and *k*, shifts behind the interstellar absorption with changing orbital phase. However, because we have no independent information concerning the intrinsic stellar Lyα core shape, we have no reason to prefer the first cross-correlation approach over the second. Accordingly, we adopted the mean shift indicated by the two approaches (the differences are only a few km s^{-1} in any event).

The interstellar Lyα registration procedure is illustrated in Figure 2 for the quadrature composite profiles based on superpositions of the 30 minute SWP exposures obtained at phases 0.27 and 0.76. The Lyα profile for phase 0.76 is shaded for clarity, and both profiles are presented in the same manner as the Mg II features of Figure 1. Although the agreement between the narrow D I absorptions is not optimum, the overall centering of the H I + D I interstellar cores appears to be reasonable, particularly since the quadrature profiles were separately registered to the conjunction profile, but not to each other. With the adopted registration, a small velocity shift is seen between the system Lyα profiles at the opposite quadratures.

Figure 3 illustrates selected emission lines from the far-ultraviolet composite spectra of Capella adjusted to the COM velocity frame assuming that the Lyα registration velocity offsets are valid for the entire echelle format (see Leckrone 1980*a*). Again, tick marks indicate the COM zero velocity at each phase. We find that the low-excitation chromospheric lines like O I and Si II are distinctly broader near the quadratures compared to the conjunctions, but they exhibit no large velocity shifts. Accordingly both of the Capella giants must contribute significantly to the composite emission in the low-excitation features. However, the high-excitation lines like C IV λ1548 and C III] λ1909 do not change shape from quadrature to conjunction, but shift bodily in radial velocity, in the same sense as the secondary star.

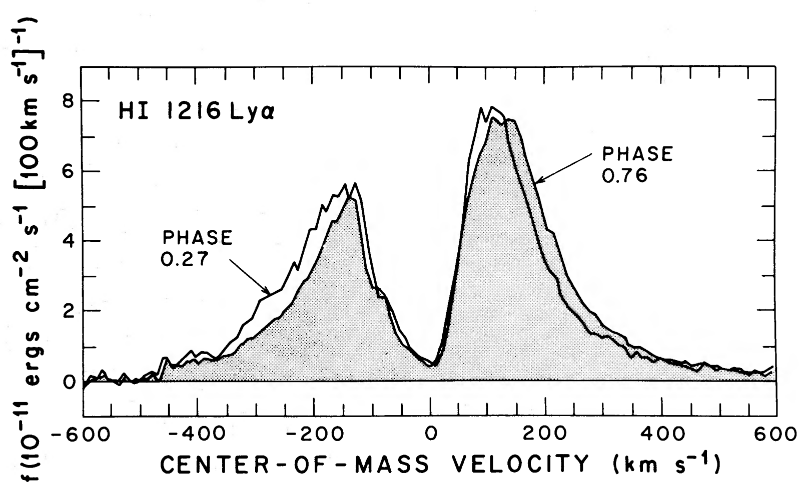

FIG. 2.—Comparison of the H I Lyα emission profile of Capella at opposite quadratures (maximum velocity separation) in the orbit, to illustrate the velocity registration procedure. Each profile is a composite of several individual 30 minute SWP exposures, plotted in the same way as the Mg II profiles of Fig. 1. Each of the quadrature composite profiles was separately registered to the interstellar absorption core of the phase 0.5 conjunction composite profile. The overall alignment of the independently registered absorption cores appears to be reasonably good. With the adopted registration of the Lyα profiles, a small velocity shift between the quadratures is evident (following the sense of the orbital motion of the secondary star).

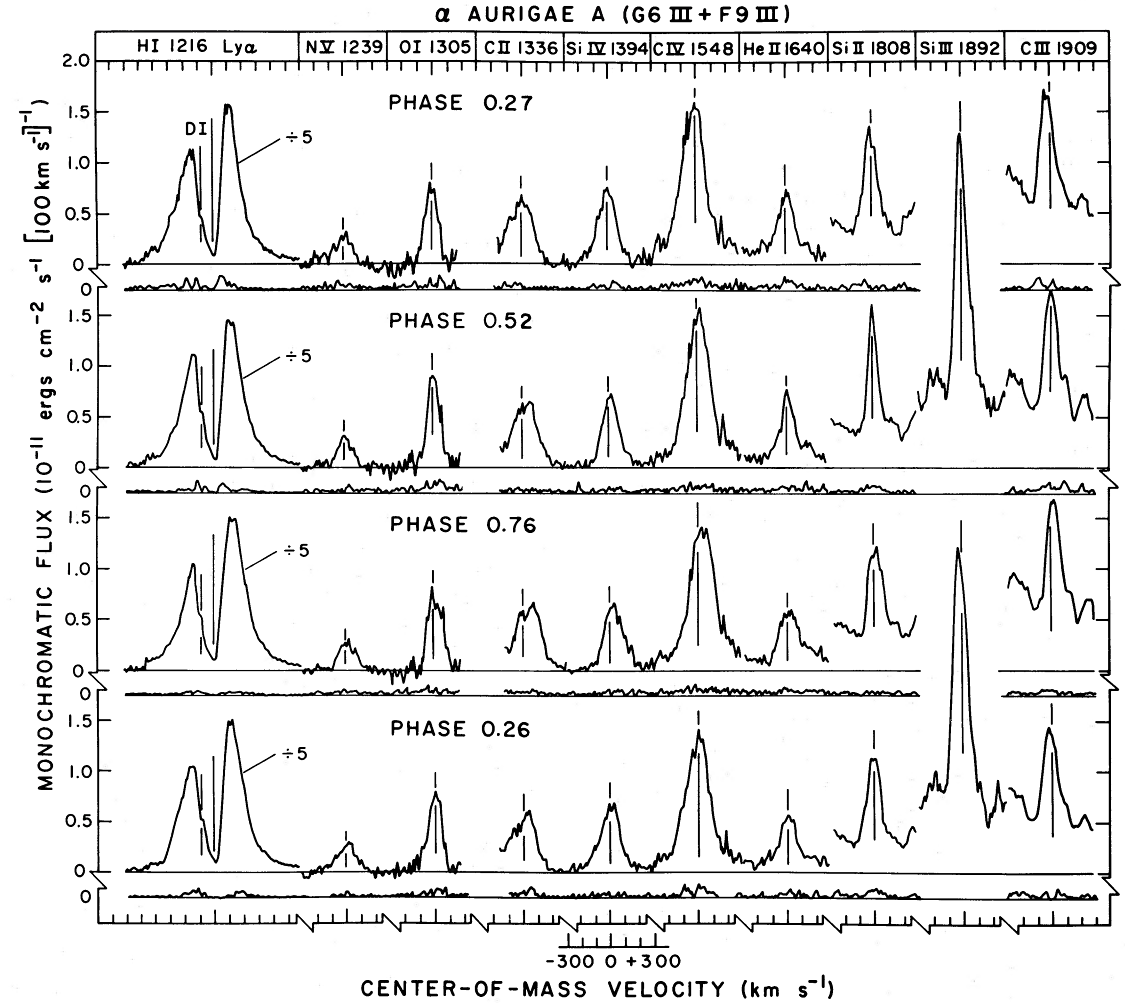

FIG. 3.—Comparison of selected emission features of the Capella far-ultraviolet spectrum at the critical orbital phases. The profiles are presented in the same manner as those of Fig. 1. RMS levels are not plotted for Si III] λ1892 because only single observations are available. The sharp emission spike longward of C IV λ1548 probably is a camera artifact ("warm" pixel) since its velocity seems to be fixed in the reference frame of the spectrograph (which changes slightly relative to the Capella COM owing to the telluric motion).

As previously noted by Ayres and Linsky (1980), the high-excitation emission from Capella must originate almost exclusively on the F-type secondary.

e) *Summary of System Spectral Properties at the Critical Phases*

Table 2 summarizes line-shape parameters for the prominent far-ultraviolet emission features based on least-squares Gaussian fits. In some cases, line fluxes were derived from direct numerical integrations. The typical uncertainty (1 σ) in the emission line centroids is $\pm 5\ \mathrm{km\ s^{-1}}$, exclusive of uncertainties in the laboratory wavelengths, while the line fluxes are reliable to the $\pm 10\%$ level, exclusive of errors in the absolute calibration itself. The table condenses the large amount of information contained in the 45 spectra obtained at the four critical phases.

First, we tabulate the COM velocities and FWHMs of emission features from the conjunction spectrum, as registered to the flux-weighted mean velocity of the chromospheric O I and Si II lines. In the next group of columns we tabulate one-half of the total velocity shift of the emission features from the phase 0.25 quadrature to the phase 0.75 quadrature and the mean FWHM at the opposite quadratures. The first quantity is the mean orbital velocity amplitude of an emission line, independent of any persistent systematic velocity shifts (see Ayres *et al.* 1983), or errors in the laboratory wavelengths. The velocity amplitude, as defined here, would be $+26\ \mathrm{km\ s^{-1}}$ for a feature emitted solely by the secondary star, and $-27\ \mathrm{km\ s^{-1}}$ for a feature emitted solely by the primary star. The phase 0.25 velocities were obtained by weighting equally the large-aperture composite spectra from phases 0.27 and 0.26, which were registered separately to the H I + D I interstellar absorption core of the phase 0.52 Lyα profile (and hence to the O I + Si II velocity normalization at the conjunction), and the single small-aperture spectrum at phase 0.27, which is on an absolute

TABLE 2

LINE SHIFTS AND WIDTHS AT CONJUNCTION AND QUADRATURE

SPECTRUM (1)	WAVELENGTH[a] (Å) (2)	$V_{0.5}$ (km s^{-1}) (3)	FWHM (4)	$\frac{1}{2}(V_{0.75} - V_{0.25})$ (km s^{-1}) (5)	FWHM (6)	f_L (10^{-12} ergs cm^{-2} s^{-1}) (7)
H I	1215.668	+2	330	11 ± 2	330 ± 10	400 ± 15
N V	1238.821	+4	130	6 ± 3	150 ± 30	4.1 ± 0.2
O I	1304.858	+1	88	7 ± 2	120 ± 10	9.0 ± 0.3
O I	1306.029	−4	94	6 ± 2	110 ± 5	10.6 ± 0.4
C II	1335.708	+18	176	20 ± 2	175 ± 10	14.2 ± 0.5
Si IV	1393.755	+10	139	15 ± 4	150 ± 10	10.7 ± 0.7
Si IV	1402.770	+6	130	14 ± 6	160 ± 20	6.7 ± 0.5
C IV	1548.185	+4	199	20 ± 2	210 ± 5	31 ± 4
C IV	1550.774	+7	180	19 ± 1	170 ± 5	17 ± 1
He II	1640.4	+10	105	3 ± 2	120 ± 10	6.3 ± 0.3
Si II	1808.012	+4	72	9 ± 1	110 ± 5	10.1 ± 0.6[b]
Si III	1892.030	−2	89	13 ± 1[c]	80 ± 15[c]	22 ± 1[b]
C III	1908.734	+0	83	20 ± 2	75 ± 5	6.4 ± 0.7[b]
Mg II	2796	...	190	...	230 ± 20	880 ± 30
Mg II	2803	...	190	...	210 ± 20	740 ± 10

NOTE.—Quantities listed in columns (3)–(7) are as follows: Column (3), centroid velocities of emission features at the phase 0.5 conjunction relative to the flux-weighted mean velocity of the Si II and O I emissions. Column (4), full width at half-maximum (FWHM) for features in the conjunction spectrum. Column (5), half the total velocity amplitude of features between the opposite quadratures. Column (6), mean FWHMs from the quadrature spectra. Column (7), mean integrated line fluxes from the four phases observed. The cited ($\pm 1\ \sigma$) uncertainties in columns (5) and (6) are based on the standard deviations about the mean of the values measured at the three quadratures. The uncertainty cited in column (7) is the standard deviation about the mean of the fluxes measured at the four orbital phases observed. There has been no correction for the 30 km s^{-1} FWHM of the instrumental profile, which has a negligible effect on the broad emission lines of the Capella ultraviolet spectrum.

[a] Kelly and Palumbo 1973.

[b] Continuum subtracted prior to Gaussian fitting.

[c] Based on values at phases 0.25 (SWP 8179 [small aperture], 11030 [large aperture]), and 0.5 (SWP 8632) only, since phase 0.75 spectra are overexposed at λ1892.

velocity scale. The small-aperture spectrum was heavily weighted in establishing $V_{0.25}$, despite its generally poor signal-to-noise, owing to the absolute wavelength calibration provided by the platinum lamp. In addition, we used the standard deviation of the three independent velocity determinations about the mean to characterize the typical measurement uncertainty, σ, at phase 0.25 *and* at phase 0.75. Accordingly, the appropriate uncertainty for one-half of the velocity difference is $(2^{1/2})/2\ \sigma$.

The final column of Table 2 lists integrated line fluxes based on the four sets of large-aperture composite spectra. The cited uncertainties are the standard deviations about the mean. The derived standard deviations generally are comparable to, and in some cases actually smaller than, the expected measurement errors estimated from the rms deviations of the empirical profiles from the fitted Gaussians, the line FWHMs, and the sampling frequency of 2.5 points per resolution element (see Landman, Roussel-Dupré, and Tanigawa 1982). The standard deviations of the line fluxes between the four observing sessions also are comparable to those of the individual profiles that were combined to form each composite, as indicated by the typical amplitude of the rms levels in Figures 1 and 2.

We conclude that Capella did not exhibit any significant line-flux variations, beyond those expected from measurement errors alone, either during the four 8 hour observing sessions, with ~1 hour time resolution, or between the first three shifts spaced at ~1 month intervals, or between the mean of the first three and the last observing opportunity, corresponding to a separation of about 9 months. Further discussion of the temporal variability of the Capella spectrum, or lack of it, based on a comprehensive 2 month ultraviolet monitoring program during the spring of 1981 will be presented elsewhere (Ayres 1983*b*).

The steadiness of the Capella emission contrasts markedly with the behavior of the cooler and less evolved subgiant primaries of short-period RS CVn systems that also are bright ultraviolet sources like Capella. For example, HR 1099 and σ Gem both have been observed twice with long SWP exposures, and in both cases changes in C IV emission levels of at least 30% between the two observations were recorded (Ayres and Linsky 1982; Ayres, Simon, and Linsky 1983). Even more dramatic changes have been observed in low-dispersion monitoring programs. For example, Marstad *et al.* (1982) discovered that II Peg is five times brighter in C IV for one-half of its orbital cycle compared with the other half, and the same authors observed an intense far-ultraviolet flare on HR 1099 during one of nine separate SWP images over two orbital cycles (~1 week).

III. ANALYSIS

The principal motivation for the present study was to derive the relative strengths of the Capella primary and secondary in representative ultraviolet emission lines in order to assess the relative chromospheric and coronal activity levels of these contemporaneous, but not necessarily coeval, giants. To accomplish this task, we numerically simulated the blended spectrum of the system to optimally match the quadrature velocity amplitude, and mean FWHMs at quadrature and conjunction, of the emission features listed in Table 2.

We modeled each prominent emission line in the Capella spectrum as a blend of two Gaussian profiles. We estimated the widths of lines from the secondary star based on the apparent FWHM of the conjunction profile and the assumption that the primary lines have the same FWHM and surface flux as those in the high-resolution spectrum of β Ceti (G9.5 III),[4] a yellow giant similar to the Capella primary in spectral type and probably also in evolutionary status (*IUE* line widths and strengths for the β Ceti spectrum were furnished courtesy of R. E. Stencel). Given the initial estimates of line widths and relative fluxes from the conjunction profiles, fitting the quadrature profiles with a blend of shifted Gaussians provided an improved estimate of the primary's flux contribution. The process was repeated until a self-consistent set of line-shape parameters was obtained for the primary and secondary star for each emission line. A similar approach was taken for the Mg II *k* line, except that we used trapezoids with central reversals instead of Gaussians to simulate the composite emission. In addition, we modelled the detailed shape of the Mg II *k* line at both quadratures, instead of adopting a mean line shape, and incorporated a narrow, stationary Gaussian absorption feature to simulate the interstellar component. The initial estimate of the Mg II *k* line shape for the primary spectrum was taken as a mean of parameters derived from the *k* lines of representative G giants from the survey of Stencel *et al.* (1980). The central reversal depth was taken from recent measurements of ϵ Vir, a late G, high-velocity giant for which the intrinsic self-reversal of the *k* line is not masked by the interstellar component (Ayres, Rodgers, and Zarro 1983).

The inferred line shape parameters for the primary and secondary star are summarized in Table 3. Also included in Table 3 are the derived surface flux ratios of the primary to the secondary, inferred normalized fluxes $f_L/l_{\rm bol}$,[5] comparisons of the normalized fluxes of the primary star to those of the yellow giants β Ceti and μ Vel, and comparisons of the secondary star to the early G active supergiant, β Dra (G2 Ib). (We computed surface fluxes and normalized fluxes for the Capella giants and the comparison stars utilizing the angular diameters and $l_{\rm bol}$ values reported by Ayres, Marstad, and Linsky 1981.)

[4] P. C. Keenan, in a private communication, has recommended that β Ceti be classified somewhat earlier than its old MK type (K1 III). An earlier classification is in accord with its "anomalous" ultraviolet continuum intensity near 1900 Å (see Ayres, Marstad, and Linsky 1981).

[5] The quantity $l_{\rm bol}$ is the stellar bolometric luminosity at Earth expressed in the same units as the line fluxes: the "normalized" fluxes are analogous to surface fluxes.

IV. DISCUSSION

The results of our program, as summarized in Table 3, confirm the earlier study of the Capella by Ayres and Linsky (1980), which was limited to orbital phases 0.50 and 0.75. Both programs found that the Capella secondary is considerably brighter than the primary, in surface flux, in all of the prominent far-ultraviolet emissions, particularly the high-excitation C II–C IV lines. The dominance of the secondary star in chromospheric activity indicators almost certainly is associated with enhanced magnetic field production resulting from its factor of ~ 6 larger rotation rate ($V_{\rm Ab} \sin i \approx 36 \pm 5$ km s^{-1}, $V_{\rm Aa} \sin i \approx 6$ km s^{-1}; F. Fekel, private communication). The large rotational velocity of the secondary in turn is likely to be related to its less advanced evolutionary state.

However, the present study has revealed several puzzling aspects of the system that were not fully appreciated in the previous work. The Capella primary indeed is fainter than the secondary in the far-ultraviolet emissions characteristic of the chromosphere and higher temperature layers, but the primary is quite comparable in normalized flux to the yellow giants β Ceti and μ Vel (see Table 3). These, in turn, are among the brightest ordinary, "single" giants in the recent C IV surveys by Simon, Linsky, and Stencel (1982) and Simon and Linsky (1982), and in the soft X-ray survey by Ayres *et al.* (1981). If one assumes for the Capella primary an $f_x/l_{\rm bol}$ ratio interpolated between those of β Ceti (40×10^{-7}) and μ Vel (80×10^{-7}) scaled as a function of either the C IV *or* He II $f_L/l_{\rm bol}$ ratios (cf. Ayres, Marstad, and Linsky 1981), then the primary would be responsible for as much as *half* of the total 0.1–4 keV soft X-ray emission from the Capella system. This is a rather unexpected result considering that the analogous ratio for C IV emission is only 10%. (Of course, owing to its smaller surface area, the secondary star would still be a factor of 3 brighter than the primary in soft X-ray surface flux.)

Our conclusion that the Capella primary is comparatively bright, for a yellow giant, in far-ultraviolet and perhaps also in soft X-ray normalized fluxes, has important implications. The fraction of "active" yellow giants agrees with the expected number of stars crossing the Hertzsprung gap for the first time from the 2–4 $M_\odot$ portion of the upper main sequence: roughly 10% according to the evolutionary tracks of Iben (1967). (The first-crossing time is about 1% of the main-sequence lifetime, compared with a postflash, helium core burning lifetime of $\sim 10\%$). The weak-emission yellow giants could then be mostly post-helium-flash, slow rotators with comparatively weak magnetic dynamos and, therefore, weak chromospheric and coronal emission. The first crossers, on the other hand, still are shedding their primordial large angular momenta, and accordingly can support

TABLE 3

COMPARISON OF DERIVED LINE PARAMETERS

					$f_L/l_{\rm bol}(10^{-7})$				
							Aa	Aa	Ab
TRANSITION	FWHM$_{\rm Aa}$[a]	$f_{\rm Aa}/f_{\rm tot}$	FWHM$_{\rm Ab}$	$F_{\rm Ab}/F_{\rm Aa}$	Aa	Ab	μ Vel (G5 III)	β Ceti (G9.5 III)	β Dra[b] (G0 Ib)
0.1–4 keV X-rays[c]	...	(0.5)[d]	...	3	[55][d]	97	0.7	1.4	3.0
N V 1239	70	0.2	160	10	1.5	9	0.6	0.8	0.7
O I 1305	70	0.3	100	5	7	26	1.0	1.2	0.3
C II 1336	60	0.1	200	25	1.7	24	0.8	1.7	1.6 [e]
Si IV 1394	50	0.1	160	25	1.4	20	0.7:	0.9	0.9
C IV 1548	90	0.1	220	25	2.7	37	0.7	2.7	1.2
He II 1640	70	0.3	130	5	1.1	4	0.5	1.8	0.6
Si II 1808	55	0.3	85	5	1.8	6	...	2.3	0.5
Si III 1892	55	[0.1][g]	[95][g]	[25]	[1.3]	18	...	[0.7]	1.0 [f]
C III 1909	60	[0.1][g]	[85][g]	[25]	[0.4]	5	...	[2.0]	0.6
Mg II 2796	(200, 60, 0.35)[h]	>0.3 <0.4 [i]	(300, 100, 0.5)[h]	<5 >4	290	<1030 <670 [j]	0.8	1.1	<1.6 >1.0

NOTE.—The typical uncertainty in the inferred $f_{\rm Aa}/f_{\rm tot}$ values from the Gaussian profile simulations is $\lesssim \pm 0.05$, *exclusive* of errors in the adopted FWHM$_{\rm Aa}$.

[a] Assumed equal to FWHM of same feature in β Ceti spectrum; from R. E. Stencel.

[b] β Dra fluxes $1200 \leq \lambda \leq 2000$ corrected for interstellar reddening according to Savage and Mathis 1979, assuming $E(B-V) = +0.16$ mag (see Stencel *et al.* 1983).

[c] $L_x = 4 \times 10^{30}$ ergs s^{-1} (Cash *et al.* 1978).

[d] Estimated from adopted $f_x/l_{\rm bol}$ value (col. [6]) as scaled from μ Vel and β Ceti (see text).

[e] Low-dispersion fluxes: Ayres, Marstad, and Linsky 1981.

[f] Values of $f_L/l_{\rm bol}$ are from high-dispersion spectra (except for μ Vel He II λ1640): β Cet courtesy R. E. Stencel; β Dra from Stencel *et al.* 1983.

[g] Assumed values since the bright structured continuum background at these features precludes an accurate assessment of profile parameters by Guassian fitting.

[h] Mg II profiles were assumed trapezoidal with triangular central reversal. Listed in parentheses are the full width at base, full width at top, and depth of central reversal.

[i] $f_{\rm tot}$ is entire flux above zero intensity between k_1 features. If one subtracts the k_1 level as a background, then the flux limits indicated in the second line are obtained ($f_{\rm Aa}$ itself is not affected since the k_1 level of Aa is negligible compared with that of Ab).

[j] Includes both Mg II components: flux integrated between k_1 or h_1 features.

substantial dynamo-generated magnetic activity and the attendent strong chromospheric and coronal emission. If this picture is correct, then the Capella primary must be among the first crossers. This would be a remarkable circumstance, because the first-crossing yellow giants are comparatively rare, and finding two within the same system would seem to be quite improbable. Nevertheless, support for this conclusion can be found in the study by Boesgaard (1971), who proposed that the Li I λ6708 absorption in the primary spectrum, which is weak but definitely present, implies that the primary has not yet ascended the red-giant branch.

If both Capella giants indeed are first crossers, and if both left the main sequence with comparable angular momenta, then the spin-down of yellow gaints in the Hertzsprung gap must be extraordinarily rapid. A similar conclusion was reached by Gray (1981) in his analysis of five G5 III stars and by Gray and Endal (1982) in their study of the Hyades K giants, which are comparable in age and mass to the Capella giants. Gray (1981) interpreted the apparent spin-down of the G giants in terms of a strong dynamo-braking phase, during which an extensive coronal wind magnetically coupled to the stellar photosphere sheds angular momentum rapidly. Gray and Endal (1982) subsequently pointed out that the apparent sharp break in rotational rates at G5 III may simply be the result of comparing first crossers to postflash stars with helium-burning cores, which presumably have had ample opportunity to shed angular momentum by a variety of mechanisms. Those authors constructed a series of models, in the spirit of the previous work by Endal and Sofia (1979), to explore possible angular momentum histories of yellow giants crossing the Hertzsprung gap for the first time. They found that evolutionary models which incorporate uniform specific angular momentum in the convective layers can reproduce the measured rotational velocities of the Hyades giants ($V_{\rm rot} \approx 3.5$ km s^{-1}) without requiring magnetic braking. Indeed, their model (case 3 in their Table 5) predicts somewhat more than a factor of 2 decrease in rotational velocity over the $\sim$230 K decrease in effective temperature from the Capella primary to the Hyades K0 giants, which is entirely compatible with the estimated equatorial rotational velocity of $\lesssim$8.5 km s^{-1} for the Capella primary (assuming that the stellar rotation is in the same plane as the binary orbit, which is inclined 137° to the line of sight).

We therefore believe that the Capella primary is near the end of its first-crossing phase prior to its initial ascent of the red-giant branch. Furthermore, the comparatively slow rotation of the Capella primary is consistent with evolutionary redistribution of angular momentum, even before considering magnetic braking by a coronal wind, thought to be the principal spindown agent for lower-main-sequence stars like the Sun (e.g., Gray 1982).

Regardless of the evolutionary status of the Capella giants, the large difference in C IV emission but possible similarity in soft X-ray luminosities is striking. Apparently, the formation of hot coronae is quite sensitive to spectral type, in addition to rotation rate. According to the correlation diagrams presented by Ayres, Marstad, and Linsky (1981), the F stars, as a class, behave anomalously in the sense that the F stars tend to have larger C IV normalized fluxes than G and K stars at similar Mg II normalized fluxes. Furthermore, in the *Einstein* survey of stellar coronae reported by Vaiana *et al.* (1981), the F stars (mostly dwarfs) have a *maximum* X-ray luminosity, L_x, similar to those of the G and K dwarfs. Since the former have larger *bolometric* luminosities than the latter, the *maximum* normalized soft X-ray flux, $f_x/l_{\rm bol}$, must be smaller for the F stars than for the cooler types, despite the substantially larger median rotational velocities of the warmer stars (e.g., Allen 1973). Nevertheless, the F stars appear to have comparatively large $f_{\rm C\,IV}/l_{\rm bol}$ ratios if the sample of the stars in the survey by Böhm-Vitense and Dettmann (1980) is representative. For example, the total emission in high-excitation lines of the far-ultraviolet spectrum of the F giant of Capella is quite similar to the 0.1–4 keV X-ray flux, whereas the corresponding ratio for the G giant is only of order 10%. Accordingly, the corona is energetically more important relative to the transition region in the cooler yellow giants like the Capella primary, whereas the 10^5 K layers emit a comparable amount of energy to the corona in the hotter stars like the Capella secondary. (Note, however, that in either situation the total radiative loss rate of the chromosphere is considerably larger than those of both the transition region and corona.)

V. CONCLUSIONS

Detailed high-dispersion ultraviolet studies of the 104 day spectroscopic binary Capella with *IUE* have revealed that *both* giants in the system quite likely have very "active" chromospheres and coronae compared with other stars in their respective spectral classes. The rapidly rotating F secondary star is considerably brighter in surface flux (or any other measure) than the moderately rotating G primary in high-excitation emissions formed near 10^5 K, like Si IV and C IV. However, the primary may be more nearly comparable to the secondary in soft X-ray surface flux, and could provide as much as *half* of the total luminosity of the system in the 0.1–4 keV band.

In retrospect, the opposite appearance of the Capella giants in different diagnostics is compatible with the general behavior of active G and F stars revealed by ultraviolet and soft X-ray surveys. In particular, the G stars tend to have much larger median X-ray-to-C IV ratios than the F stars. Since the median rotational velocity among the F stars is larger than among the G types, the X-ray rotation-activity connection must exhibit a much greater sensitivity to spectral type, and hence to convection zone parameters, than does the C IV rotation-activity connection.

In this regard, the large contrast in rotation rates between the primary and secondary of Capella is compatible with the angular momentum redistribution and rapid spin-down that accompanies the evolution of a $\sim 2.5\ M_\odot$ giant through the Hertzsprung gap for the first time (cf. Gray and Endal 1982). The indirect indicators of first-crossing status for both Capella giants supports Boesgaard's (1971) original suggestion to that effect based on high-dispersion studies of the lithium content of the Capella giants. In this context the differences in activity levels of the four K giants of the Hyades (Baliunas, Hartmann, and Dupree 1981) is easy to accept, since the Capella giants, which are precursors to the evolutionary state of the Hyades giants, demonstrate that a small difference in evolutionary status in the Hertzsprung gap can lead to an enormous contrast in ultraviolet emission levels.

VI. FURTHER STUDY

Much of the discussion in § IV was based on inferences derived from analysis of the composite line shapes of ultraviolet emission features observed at critical phases in the Capella orbit. The limited spectral resolution and signal-to-noise of the *IUE* spectrographs and vidicons are not likely to permit dramatic improvements in that class of analysis for the foreseeable future. However, quantitative and qualitative improvements are expected with the High Resolution Spectrograph on Space Telescope (Leckrone 1980*b*).

Furthermore, Capella offers a unique target for future soft X-ray monitoring efforts. In particular, the total X-ray flux from the system should be modulated at the 8 ± 1 day rotational period of the secondary star, and at the ~ 75 day rotational period of the primary. The respective modulation depths, compared with the expected relative contribution to the total flux, should indicate the degree of homogeneity of magnetic flux on the two giants. Such modulation studies could be the forerunners of high-resolution maps of the system obtained with X-ray interferometers or direct imaging techniques (the separation is about 50 milli-arcsec, while the angular diameters are about 8 and 5 milli-arcsec for the primary and secondary, respectively.) These studies would provide a unique opportunity to investigate the spatial organization of magnetic fields on two stars of different spectral type, but otherwise similar properties.

A second area of importance for future work is the evolutionary status of the system. The present study reemphasizes the possibility, originally suggested by Boesgaard, that both of the Capella giants are crossing the Hertzsprung gap for the first time. If true, the masses of the Capella giants must be even closer than the 5% difference indicated by Wright's (1954) detailed study of the primary and secondary spectra. Otherwise, the two yellow giants should not be found in nearly the same position in the H-R diagram, unless our understanding of the first-crossing phase is quite deficient. To establish the relative masses of the Capella giants accurately, one must be able to monitor the orbital radial velocities with great precision. This is a difficult undertaking in the *IUE* composite spectrum owing to the problem of blending aggravated by the rotational broadening of the secondary spectrum. The blending problem would be eliminated if the two stars could be observed individually. For example, the combination of speckle interferometry techniques with dispersive spectroscopy—speckle-spectroscopy (see, e.g., Butcher, Joseph, and Timothy 1982)—might permit the radial velocities of the two components to be isolated near the elongations, and thereby help establish the relative masses and evolutionary status of the system more precisely.

Finally, we recall the pioneering study of the Capella optical spectrum by Wright (1954), who applied a mechanical subtraction procedure to isolate the secondary spectrum relative to an assumed primary spectrum, much as β Ceti was utilized in this work. Ironically, the closest match Wright found to the optical absorption spectrum of the primary was β Dra, the somewhat reddened early G supergiant whose ultraviolet properties—line widths and surface fluxes (see Stencel *et al.* 1983)—most closely resemble those of the Capella *secondary*.

We thank the staff of the *IUE* Observatory for their help in the acquisition of the stellar spectra described in this study, and Dr. T. Simon for obtaining the observations at phase 0.26. We also thank the staff of the *IUE* Regional Data Analysis Facility in Boulder operated under grant NAS5-26409 for their help in the reduction of some of these data. We acknowledge support by grants NAG5-199, NAG-82 and NGL-06-003-057 from the National Aeronautics and Space Administration to the University of Colorado.

REFERENCES

Allen, C. W. 1973, *Astrophysical Quantities* (3d ed.; London: Athlone).
Ayres, T. R. 1983*a*, *IUE Newsletter*, submitted.
———. 1983*b*, in preparation.
Ayres, T. R., and Linsky, J. L. 1980, *Ap. J.*, **241**, 279.
———. 1982, *Ap. J.*, **254**, 168.
Ayres, T. R., Linsky, J. L., Vaiana, G. S., Golub, L., and Rosner, R. 1981, *Ap. J.*, **250**, 293.
Ayres, T. R., Marstad, N. C., and Linsky, J. L. 1981, *Ap. J.*, **247**, 585.
Ayres, T. R., Rodgers, A. W., and Zarro, D. 1983, in preparation.
Ayres, T. R., Simon, T., and Linsky, J. L. 1983, *Ap. J.*, (*Letters*), submitted.
Ayres, T. R., Stencel, R. E., Linsky, J. L., Simon, T., Jordan, C., Brown, A., and Engvold, O. 1983, *Ap. J.*, submitted.
Baliunas, S., Hartmann, L., and Dupree, A. K. 1981, in *The Universe at Ultraviolet Wavelengths: The First Two Years of IUE*, ed. R. D. Chapman (NASA Conf. Publ. 217), p. 325.
Batten, A. H., Fletcher, J. M., and Mann, P. J. 1978, *Pub. Dom. Ap. Obs.*, **15**, 121.
Beeckmans, F., and Penston, M. 1979, *IUE* Three-Agency Meeting Report.
Boesgaard, A. M. 1971, *Ap. J.*, **167**, 511.
Boggess, A., *et al.* 1978, *Nature*, **275**, 377.
Böhm-Vitense, E. 1981, *Ap. J.*, **244**, 504.
Böhm-Vitense, E., and Dettmann, T. 1980, *Ap. J.*, **236**, 560.
Butcher, H. R., Joseph, C. L., and Timothy, J. G. 1982, in *SPIE Instrumentation in Astronomy IV*, Vol. **331**, in press.
Cash, W., Bowyer, S., Charles, P., Lampton, M., Garmire, G., and Riegler, G. 1978, *Ap. J.* (*Letters*), **223**, L21.
Cassatella, A., Ponz, D., and Selvelli, R. L. 1981, *IUE Newsletter*, No. 14, p. 270.
Dupree, A. K., Baliunas, S. L., and Shipman, H. 1977, *Ap. J.*, **218**, 361.
Endal, A. S., and Sofia, S. 1979, *Ap. J.*, **232**, 531.
Gray, D. F. 1981, *Ap. J.*, **251**, 155.
———. 1982, preprint.
Gray, D. F., and Endal, A. S. 1982, *Ap. J.*, **254**, 162.
Iben, I., Jr. 1965, *Ap. J.*, **142**, 1447.
———. 1967, *Ann. Rev. Astr. Ap.*, **5**, 571.
Kelly, R. L., and Palumbo, L. J. 1973, *Atomic and Ionic Emission Lines below 2000 Angstroms* (NRL Report 7599).
Landman, D. A., Roussel-Dupré, and Tanigawa, G. 1982, *Ap. J.*, **261**, 732.
Leckrone, D. S. 1980*a*, *IUE Newsletter*, No. 10, p. 25.
———. 1980*b*, *Pub. A.S.P.*, **92**, 5.
Marstad, N., *et al.* 1982, in *Advances in Ultraviolet Astronomy: Four Years of IUE Research*, ed. Y. Kondo, J. M. Mead, and R. D. Chapman (NASA Conf. Pub. 2238), p. 554.
Parker, E. N. 1970, *Ann. Rev. Astr. Ap.*, **8**, 1.
Savage, B. D., and Mathis, J. S. 1979, *Ann. Rev. Astr. Ap.*, **17**, 73.
Simon, T., and Linsky, J. L. 1982, in *Advances in Ultraviolet Astronomy: Four Years of IUE Research*, ed. Y. Kondo, J. M. Mead, and R. D. Chapman (NASA Conf. Pub. 2238), p. 273.
Simon, T., Linsky, J. L., and Stencel, R. E. 1982, *Ap. J.*, **257**, 225.
Stencel, R. E., Linsky, J. L., Ayres, T. R., Jordan, C., and Brown, A. 1983, *Ap. J.*, submitted.
Stencel, R. E., Mullan, D. J., Linsky, J. L., Basri, G. S., and Worden, S. P. 1980, *Ap. J. Suppl.*, **44**, 383.
Turnrose, B. E., and Bohlin, R. C. 1981, *IUE Newsletter*, No. 13, p. 1.
Turnrose, B. E., Thompson, R., and Bohlin, R. 1982, *IUE Newsletter*, No. 18, p. 21.
Vaiana, G. S., and Rosner, R. 1978, *Ann. Rev. Astr. Ap.*, **16**, 393.
Vaiana, G. S., *et al.* 1981, *Ap. J.*, **245**, 163.
Wallerstein, G. 1966, *Ap. J.*, **143**, 823.
Wright, K. O. 1954, *Ap. J.*, **119**, 471.

Thomas R. Ayres: Laboratory for Atmospheric and Space Physics, Campus Box 392, University of Colorado, Boulder, CO 80309

Jeffrey L. Linsky: Joint Institute for Laboratory Astrophysics, Campus Box 440, University of Colorado, Boulder, CO 80309

Francis H. Schiffer III: Astronomy Department, Computer Sciences Corporation, Silver Spring, MD 20910